De Novo Design of a Tumor-Penetrating Peptide

Luca Alberici[1,2,3], **Lise Roth**[4], **Kazuki N. Sugahara**[1], **Lilach Agemy**[1], **Venkata R. Kotamraju**[1], **Tambet Teesalu**[1], **Claudio Bordignon**[2,3], **Catia Traversari**[2], **Gian-Paolo Rizzardi**[2], and **Erkki Ruoslahti**[1]

[1]Cancer Center, Sanford-Burnham Medical Research Institute, 10901 N. Torrey Pines Rd., La Jolla, CA 92037 U.S.A. and Center for Nanomedicine, University of California, Santa Barbara, CA 93106-9610

[2]MolMed S.p.A., Via Olgettina 58, 20132 Milano, Italy

[3]Università Vita-Salute San Raffaele, Via Olgettina 58, 20132 Milano, Italy

[4]Division of Vascular Oncology and Metastasis, German Cancer Research Center (DKFZ), Im Neuenheimer Feld 280, 69120 Heidelberg, Germany

Abstract

Poor penetration of anti-tumor drugs into the extravascular tumor tissue isoften a major factor limiting the efficacy of cancer treatments. Our group has recently described a strategy to enhance tumor penetration of chemotherapeutic drugs through use of iRGD peptide (CRGDK/RGPDC). This peptide comprises two sequence motifs: RGD, which binds to $\alpha v \beta 3/5$ integrins on tumor endothelia and tumor cells and a cryptic CendR motif (R/KXXR/K-OH). Once integrin binding has brought iRGD to the tumor, the peptide is proteolytically cleaved to expose the cryptic CendR motif. The truncated peptide loses affinity for its primary receptor and binds to neuropilin-1, activating a tissue-penetration pathway that delivers the peptide along with attached or co-administered payload into the tumor mass. Here we describe the design of a new tumor-penetrating peptide based on the current knowledge of homing sequences and internalizing receptors. The tumor-homing motif in the new peptide is the NGR sequence, which binds to endothelial CD13. The NGR sequence was placed in the context of a CendR motif (RNGR), and this sequence was embedded in the iRGD framework. The resulting peptide (CRNGRGPDC, iNGR) homed to tumor vessels and penetrated into tumor tissue more effectively than the standard NGR peptide. iNGR induced greater tumor penetration of coupled nanoparticles and co-administered compounds than NGR. Doxorubicin given together with iNGR was significantly more efficacious than the drug alone. These results show that a tumor-specific, tissue-penetrating peptide can be constructed from known sequence elements. This principle may be useful in designing tissue-penetrating peptides for other diseases.

Keywords

Tissue-penetrating peptide; C-end Rule; NGR; Tumor targeting; Drug delivery

---

Corresponding Author: Erkki Ruoslahti, Distinguished Professor, Cancer Center, Sanford-Burnham Medical Research Institute, 10901 N. Torrey Pines Rd., La, Jolla, CA 92037 U.S.A., Phone: 858 795-5023, ruoslahti@sanfordburnham.org.

Introduction

The vasculature of each tissue is unique in terms of protein expression and these molecular differences are referred to as "vascular zip codes"(1). The selectively expressed proteins provide targets for specific delivery of diagnostic and therapeutic compounds to the vasculature of desired tissues. Currently, a variety of tumor-targeting peptides are in preclinical and clinical development. However, vascular abnormalities, fibrosis and contraction of extracellular matrix contribute to an increased interstitial fluid pressure inside the tumor, which impedes drug delivery into the extravascular tumor tissue (2).

Our group has recently reported the identification of the CendR motif (R/KXXR/K) that is capable of increasing the penetration of peptides, chemicals, and synthetic and biological nanoparticles into tissues through the engagement of neuropilin-1 (NRP-1) (3). Specific penetration into tumors was achieved through the use of an iRGD peptide (CRGDK/RGPDC)(4). iRGD, identified by *in vivo* phage display for tumor homing peptides, combines targeting to tumor vessels and tumor parenchyma through an RGD motif with the cell-internalizing and tissue penetrating properties of a CendR motif RGDK/R in the peptide (4). iRGD mechanism of action involves three steps. First, the RGD sequence binds to $\alpha v \beta 3/5$ integrins. Then, a proteolytic cleavage by a yet-to-be-identified host protease(s) exposes the CendR motif, which is now able to interact with NRP-1 to trigger the internalization process. This strategy allows the activation of the CendR motif only in a targeted tissue, avoiding NRP-1 activation in normal vasculature. Interestingly, iRGD triggers a specific tumor penetration of, not only iRGD-coupled compounds, but also of drugs co-administered with free iRGD peptide (5).The CendR motif also activates the penetration pathway through binding to NRP-2 (6).

Potentially, the addition of a cryptic CendR motif could increase the penetration of other tumor targeting peptides, providing more tools to overcome the poor delivery of drugs to tumors. We set out to test this hypothesis using the NGR tumor-homing motif. The NGR sequence was identified by *in vivo* phage display in tumor bearing mice (7). Initially it was thought to bind one or more of the integrins selectively expressed in angiogenic vessels (7, 8). This idea was further supported by the discovery that the asparagine in the NGR motif undergoes a spontaneous deamidation reaction that yields iso-aspartic acid (isoDGR), generating an RGD mimetic(9, 10). However, the unaltered NGR motif also specifically homes to tumor vessels, where it binds to an isoform of amino peptidase N (CD13)(11, 12). NGR peptides have been used to target a variety of agents into tumors; an NGR conjugate of human tumor necrosis factor α is in advanced clinical trials for cancer therapy (13–16). Here we combined the NGR motif with a CendR motif to create a new tumor-homing peptide with tissue-penetrating properties.

Materials and Methods

Animal use

All procedures on the animals, including those to ensure minimizing discomfort, have been carried out according to the protocol approved at the Sanford-Burnham Medical Research Institute.

Preparation of compounds

Synthetic peptides (4), peptide-coated NWs (17) and peptide-expressing T7 phage (18) were prepared as described elsewhere. DOX was purchased from Sigma-Aldrich (St. Louis, MO). Evans Blue was purchased from MP Biomedicals (Irvine, CA)

Cell lines and tumor models

HUVECs (Lonza, Allendale, NJ) were cultured in complete EGM-2 medium from Lonza. 4T1 cells were cultured in Dulbecco's Modified Eagle Medium (Thermo Scientific, Rockford, IL) supplemented with 10% fetal bovine serum (FBS) and penicillin/streptomycin (Gibco, Grand Island, NY). All tumor cell lines were bought and authenticated by ATCC (Teddington, UK). Orthotopic 4T1 breast tumors were generated by injecting 10^5 cells into the mammary fat pad of female BALB/c mice at the age of 4–6 weeks (Harlan Sprague-Dawley, Indianapolis, IN).

In vitro phage binding and internalization assays

Phage amplification, purification, titration, sequencing, and UV inactivation were performed as reviewed (18). One million cells were incubated with 10^{10} plaque forming unit (pfu) of purified phage in DMEM-1% BSA at 4°C for binding or 37°C for internalization. The cells were washed with cold DMEM-BSA four times, lysed in lysogeny broth (LB) containing 1% Nonidet P-40 (LB-NP40) and titrated. In internalization assays, the second wash was replaced with an acid wash (500 mMNaCl, 0.1 M glycine, 1% BSA, pH 2.5) to remove and inactivate phage bound to the cell surface. In inhibition assays, the cells were incubated with 1 μg/ml of neutralizing anti-NRP-1 antibody (R&D Systems), control IgG (Santa Cruz Biotechnology), or 10-fold excess of UV-inactivated phage 15 min prior to adding the phage of interest.

Ex vivo tumor dipping assays

The assays were performed as described elsewhere (5, 6). Briefly, 4T1 tumor bearing mice were anesthetized and perfused through the heart with PBS containing 1% BSA. The tumors were excised and incubated with 10^9 pfu of phage in DMEM-1% BSA for 1 hour at 37°C. After extensive washes with PBS, the tumors were lysed in 1 ml of LB-NP40 for phage titration. In some cases, the tumors were fixed in PBS containing 4% paraformaldehyde (PFA) and processed for immunostaining.

Biodistribution of peptides, phage and NWs

In vivo tumor homing experiments with peptides, phage, and NWs were performed as described (4, 17). Briefly, 10^9 pfu of phage particles were injected into the tail vein of tumor bearing mice, and allowed to circulate for 40 minutes. The mice were perfused through the heart with PBS containing 1% BSA under deep anesthesia. The tumors and tissues were excised and mechanically homogenized for phage titration or fixed in 4% PFA for immunostaining. In some cases, 50 μg of anti-NRP-1 antibody or control IgG was intravenously injected 15 minutes prior to the phage injection. For the peptide homing studies, 100 μl of 1 mM FAM-labeled peptides were intravenously injected into tumor mice and allowed to circulate for 1 hour. In case of the NWs, particles at a dose of 5 mg/kg of iron were injected into the tail vein of tumor mice and allowed to circulate for 5 hours. After perfusion of the mice, tissues were collected, macroscopically observed under UV light (Illuminatool Bright Light System LT-9900), and processed for immunostaining. Intratumoral accumulation of NWs was quantified with Image J.

Immunofluorescence

Immunofluorescence on cells was performed using 10 μM FAM-peptides and following the protocol previously described (19). Immunofluorescence on frozen sections was performed as described earlier (4) using the following antibodies at 1:200 dilution: rat anti-mouse CD31 Alexa-594 (Invitrogen), rabbit anti-T7 phage (3) and donkey anti-rabbit Alexa 488 (Invitrogen). Images were taken using a Fluoview confocal microscope (Olympus, Center Valley, PA).

In vivo systemic permeability assay

Tumor bearing mice were injected intravenously with 4 μmol/kg of peptide combined with 1 mg of Evans Blue, 10 mg/kg of free DOX or 5 mg iron/kg of CGKRK-coated NWs (20). After indicated time of circulation, the mice were perfused through the heart with PBS supplemented with 1% BSA, and tissues were collected. Evans Blue was extracted by incubating the tissues in 1 ml of 2,2 N-methylformamide overnight at 37°C with mild shaking. After centrifugation, the OD_{600} of the supernatant was measured. To assess the extravasation of CGKRK-NWs, tissues were fixed in 4% PFA overnight at 4°C and subjected to immunostaining for CD31-positive blood vessels. For DOX quantification (21), excised tissues were mechanically homogenized in 1 ml of 1% Sodium Dodecyl Sulphate (SDS) containing 1 μM H_2SO_4 and frozen overnight in 2 ml of chloroform/isopropyl alcohol (1:1, v/v). The samples were melted, vortexed and centrifugated at 16,000 g for 15 min, and OD_{490} of the organic (lower) phase was measured.

Tumor treatment studies

Mice bearing orthotopic 4T1 breast tumors at 50 mm^3 received intravenous injections of free DOX (3 mg/kg) or PBS, combined with 4 μmol/kg of peptide every other day. Tumor growth and body weight were monitored every other day. The tumor volume was calculated using the following formula: volume (mm^3) = ($d^2 \times$D)/2, where d is the smallest and D is the largest tumor diameters.

Statistical analysis

All data were analyzed with one-way ANOVA. Tumor treatment studies were analyzed with two-way ANOVA for repeated measurements.

Results

Design of iNGR peptide

We used 3 elements to create the iNGR peptide (CRNGRGPDC): the NGR motif, a CendR motif (RNGR) overlapping with the NGR motif, and a cleavable consensus (GPD) from the iRGD peptide. The cyclic conformation required for high affinity binding of NGR to CD13 (22)was obtained through the addition of cysteines at the N- and C- terminus of the peptide. We also prepared the truncated version of iNGR that is expected to result from proteolytic activation of iNGR (CRNGR), which we refer to as iNGRt. The conventional NGR (CNGRC), RGD (CRGDC),iRGD (CRGDKGDPC) and activated iRGD (CRGDK) peptides were used as controls. The peptides used in this study are summarized in Table S1.

iNGR and NGR bind to the same primary receptor

Human umbilical vein endothelial cells (HUVECs) express on their surface both the NGR receptor CD13 and the CendR receptor NRP-1 (Fig S1). iNGR bound to HUVECsas efficiently as CNGRC, whether tested as FAM-labeled peptide (Fig. 1A) or displayed on phage (Fig. 1B, black columns). As expected, the iNGR phage did not bind $CD13^+$ U937 monocytes (Fig. S2A-C), as previously reported for the CNGRC peptide (11). UV-inactivated phage displaying CNGRC inhibited the HUVEC binding of the iNGR phage in a dose-dependent fashion, whereas inactivated CRGDC did not differ from insertless control phage in this regard (Fig. 1C). CNGRC phage did not inhibit the binding of iRGD phage to HUVECs (Fig. S3A). Moreover, only *in vitro* deamidated CNGRC and iNGR phage showed binding to immobilized αvβ3 integrin (Fig. S3B). These results suggest that CNGRC and iNGR bind to the same primary receptor through the NGR motif and that the conversion of asparagine to aspartate does not take place during phage production, purification, storage, or

during the incubations. Therefore the binding of CNGRC and iNGR to cells is not due to isoDGR interacting with $\alpha v\beta 3/5$ integrins.

The iNGRCendR motif interacts with NRPs and promotes cell internalization

We constructed phage displaying a truncated version of iNGR in which the CRNGR CendR motif occupies a C-terminal position (iNGRt). This phage bound avidly to HUVECs, likely due to an interaction with NRP-1 (Figs. 1A and 1B). Indeed, iNGRt phage binding to HUVECs was reduced by pre-incubation with a UV-inactivated phage expressing a prototypic CendR motif peptide (RPARPAR) or a neutralizing NRP-1 antibody (Fig. 1B), indicating involvement of the CendR/NRP-1 pathway. Pre-incubation with a phage displaying a peptide with a blocked CendR motif (RPARPARA),and a control antibody, had no effect on iNGRt binding to HUVECs. The binding of intact iNGR was not affected by the UV-inactivated RPARPAR phage or NRP-1 antibody showing thatNRP-1is not involved in the initial binding of the peptide. Measuring phage internalization by incubating phage with HUVECs at 37°C, followed by a wash with a low pH buffer to inactivate extracellular phage, showed stronger internalization of iNGR and iNGRt than CNGRC (Fig. 1D). Inhibition experiments showed that the internalization was mediated by the interaction of the CendR motif with NRP-1. These results suggest that HUVECs express a protease capable of activating the cryptic CendR motif embedded in the iNGR peptide. Indeed, massspectrometry showed that upon incubation of HUVECs with FAM-iNGR peptide, only the cleaved FAM-CRNGR fragment (m/z: 1076.527), but not the full-length peptide (m/z: 1445.065), was present inside the cells (Fig S4). FAM-CNGRC peptide (m/z: 1020.020) did not penetrate into the cells. Direct proof that the CendR motif within the iNGR peptide iscapable of binding to NRPs was provided by CRNGR phage binding to immobilized NRP-1 (Fig. 1E). This phage also bound to NRP-2 (Fig. 1F). In agreement with the finding that the motif R/KXXR/K has to be in a C-terminal position to bind to NRPs (the Cend-Rule)(3), only phage expressing the iNGRt, and the analogous iRGDt, bound to the NRPs, whereas the corresponding full-length peptides showed only background binding. Interestingly, iNGRt showed higher affinity for NRP-1 and NRP-2 than iRGDt, suggesting that a C-terminal arginine residue (CRNGR) provides higher affinity than lysine (CRGDK).

iNGR penetrates deeper into tumors than NGR

We have previously shown in *ex vivo* tumor penetration assays that iRG Dutilizes a CendR-mediated active transport system to cross tumor barriers (5). To investigate the iNGR-mediated penetration pathway, we performed an *ex vivo* tumor penetration assay of phage using explants of orthotopic4T1 murine breast tumors (positive for expression of CD13 and NRP1/2; Fig 2A). To evaluate the extent of tumor penetration, we titrated the phage recovered from tumors (Fig 2B) and determined the distribution of phage immunoreactivity (Fig 2C). The CendR-containing phage (iNGR and iRGD) penetrated into the explants with similar patterns, whereas non-CendR phage (CNGRC and control) remained at the outer rim of the explants. These results suggest that iNGR and iRGD share a similar CendR-mediated transport mechanism to penetrate tumor tissue.

Systemic iNGR selectively accumulates and penetrates into tumors

Having determined that the CendR motif within the iNGR peptide can be proteolytically activated to trigger interaction with NRPs and penetration into cells and tissues, we assessed the homing of iNGR *in vivo*. Intravenously administered iNGR phage accumulated within the tumor and penetrated into the tumor stroma more than CNGRC phage (Fig 3A and B upper panels). The iNGRt phage also showed high tumor penetration, presumably because of the high expression of NRP-1 on tumor vasculature and tumor cells, but this phage also accumulated in lungs and heart of the tumor mice. iNGR penetration could be blocked by concomitantly administering a neutralizing anti-NRP-1 antibody, but not a control antibody

(Fig 3B lower panels).Vascular targeting of iNGR was not inhibited by the anti-NRP-1 treatment (arrows, Fig 3B left lower panel), supporting the notion that the CendR activation occurs after iNGR accomplishes NGR-dependent vascular targeting. Intravenously injected FAM-iNGR peptide also accumulated in 4T1 breast tumors (Fig. 3C) and BxPC-3 pancreatic tumors (Fig. S5A) more strongly than FAM-CNGRC. FAM-iNGR extravasation within tumor tissue was greater than that of FAM-CNGRC (Fig 3D). FAM-iNGR selectively penetrated into tumors and not into control organs (Fig 3E). Elongated iron oxide nanoparticles (nanoworms; NWs) coated with iNGR also showed higher extravasation than CNGRC-NWs (Fig 3F and S5B). The NWs wereless efficient than phage in penetrating the tissue, likely because they are larger in size (NWs, 30×70/200 nm; phage, 55nm).

iNGR triggers tumor-specific penetration of co-administered compounds

The engagement of NRP-1 increases vascular permeability (23), and iRGD triggers this phenomenon specifically in tumors (5). We found that iNGR significantly increased extravasation and accumulation of the albumin-binding dye Evans blue in 4T1 tumors, but not in non-tumor tissues. CNGRC or vehicle alone had no effect on the biodistribution of the dye (Fig. 4A, 4B, and S6). iNGR facilitated tumor-specific accumulation of Evans bluein CT26 colon and LLC lung tumor models as well(Fig. S7). We also co-administered iNGR with NWs coated with a tumor homing peptide, CGKRK (20) which brings the NWs to tumor vessels, but does not trigger extravasation. iNGR allowed the NWs to extravasate into the tumor parenchyma (Fig. 4C). Finally, iNGR triggered more penetration of doxorubicin (DOX)into the tumors than DOX alone or DOX combined with CNGRC (Fig. 4D).

iNGR enhances anticancer drug efficacy

Having found that iNGR co-administration increased the local accumulation of DOX within tumors, we investigated the effect of iNGR on the activity of DOX. We treated orthotopic4T1 breast tumor mice with a combination of DOX (3 mg/kg) and 4 μmol/kg of iNGR, a control peptide, or PBS every other day. As shown in Figure 5A, iNGR, but not CNGRC, enhanced the antitumor effect of DOX. iNGR alone had no effect on tumor growth. Loss of body weight as an indicator of DOX toxicity was not affected by the peptide co-administration (Fig. 5B). These results demonstrate the potential of iNGR as an adjuvant to increase the efficacy of co-administered anticancer drugs.

Discussion

We report here the design of a new tumor-penetrating peptide, iNGR. The peptide was constructed by combining the tumor-targeting motif NGR and tissue-penetrating CendR motif into a 9-amino acid cyclic peptide. The iNGR peptide, homed to tumor vessels, exited the vessels, and penetrated into the tumor mass. It was able to take both coupled and co-administered payloads with it. When the co-administered payload was a drug (DOX), the efficacy of the drug increased. These results show that it is possible to use the existing knowledge to construct a new tumor-specific, tissue-penetrating peptide.

The mechanisms underlying iNGR activity are similar to those described for iRGD(4, 5). The receptor for the tumor-targeting motif NGR is a variant form of aminopeptidase N (12). The binding of iNGR to cultured cells was specifically inhibited by CNGRC, indicating that iNGR binds to the same receptor. NGR peptides are known to spontaneously undergo slow deamidation of the asparagine residue into isoaspartic acid. The resulting isoDGR peptides, like RGD peptides, bind to αv integrins. Our results exclude integrin involvement in the binding of iNGR peptide and phage to cultured cells. It is also unlikely that isoDGR formation affects the *in vivo* tumor targeting of iNGR because the deamidation process takes several hours (24), whereas the half-life of intravenously injected peptides of the size of

iNGR is only minutes(25). Thus iNGR and iRGD bind to different primary receptors on cells.

Upon engagement of the iRGD peptide at the plasma membrane of target cells, a proteolytic cleavage by a yet-to-be-identified enzyme(s) exposes the CendR sequence, which subsequently binds to NRP-1 (4). Our evidence indicates that the same mechanism operates with iNGR. First, phage displaying the predicted CendR product of iNGR, CRNGR (iNGRt) bound to NRP-1 and NRP-2, and did so with a higher affinity than CRGDK fragment of iRGD. The reason for the difference may be that a peptide with a C-terminal arginine binds more efficiently to NRPs than a peptide with a lysine C-terminus (26). Comparison of the tumor-homing efficacy of iRGD with an arginine or a lysine (CRGDK/RGPDC) showed that the lysine-containing form was more effective *in vivo* (4). It may be that other effects of the lysine residue, such as stronger integrin binding or higher susceptibility to protease cleavage, overcome the effect of lower affinity for NRPs. Second, iNGR, both as a synthetic peptide and on phage was taken up by cells in a NRP-dependent manner. Third, we isolated the iNGRt CendR fragment from inside cells treated with the intact iNGR peptide, as has been previously done with iRGD(4). Fourth, the co-injection of iNGR phage with neutralizing anti-NRP-1 antibody resulted in a reduced extra vasation of iNGR. These results show that iNGRt, the active form of iNGR, is generated through proteolysis and that the tumor-penetrating properties of iNGR are based on its ability to activate the CendR pathway.

The activation of iNGR into iNGRt appears to take place only in tumors because iNGR only accumulated in tumors. In contrast, the truncated iNGRt form, while showing preferential homing to tumors, also accumulated in the lungs and heart. This homing pattern reflects the expression of NRP-1, which is universal in the blood vessels but particularly high in tumor vessels (27).The reason for the selective activation of the cryptic CendR motif in tumors is likely to be that binding to the primary receptor is needed for the activating proteolytic cleavage. Previous work from our laboratory has shown that an iRGD variant that does not bind to integrins, but contains a CendR motif, does not penetrate into cultured cells, whereas iRGD does (4). The nature of the primary receptor does not seem to matter, as long as the receptor is tumor specific. iRGD and iNGR bind to different primary receptors, but both become activated in cell cultures and in tumors. Moreover, we have recently shown that a previously identified tumor-homing peptide, CGNKRTRGC (LyP-1)(28)also penetrates into tumors through the CendR/NRP mechanism (6). The primary receptor for this peptide is p32/gC1qR/ HABP1, a mitochondrial protein expressed at the cell surface in tumors (29). Thus, our results show that at least 3 different primary receptors can initiate the sequence of events that leads to the NRP-dependent activation of the CendR pathway in tumors. Importantly, the difference in the primary receptors allows us to differentially target tumors or tumor areas based on receptor expression patterns, providing multiple options to enhance tumor therapy with tumor-specific CendR peptides.

The experiments with phage, fluorophore-labeled peptide, and nanoparticles showed the ability of iNGR to take coupled payloads into the extravascular tumor tissue. Our results further demonstrate that such enhanced delivery and tumor penetration also applies to compounds co-administered with iNGR. Importantly, we showed this for DOX, the anti-tumor activity of which was increased by injecting the drug together with iNGR.

The co-administration strategy has significant advantages. First, because chemical coupling is not needed, new chemical entities are not created, providing a faster route for clinical development. Second, unlike targeting of compounds chemically coupled to an homing element, the co-administration process is not strictly dependent on the number of available receptors, which seriously limits the amount of a drug that can be delivered to a target (30).

Taken together, our results show that iNGR possesses the same targeting ability as CNGRC, supplemented with cell-internalizing and tumor-penetrating properties. This transformation suggests an important principle: a targeting peptide can be *ad hoc* improved by the addition of a CendR motif, which endows the peptide with tissue-penetrating properties and allows enhanced delivery of co-administered compounds into a target tissue. Rational optimization of targeting peptides in this manner may also have valuable applications in other diseases.

Supplementary Material

Refer to Web version on PubMed Central for supplementary material.

Acknowledgments

References

1. Ruoslahti E. Specialization of tumour vasculature. Nat Rev Cancer. 2002; 2:83–90. [PubMed: 12635171]

2. Heldin CH, Rubin K, Pietras K, Ostman A. High interstitial fluid pressure - an obstacle in cancer therapy. Nat Rev Cancer. 2004; 4:806–813. [PubMed: 15510161]

3. Teesalu T, Sugahara KN, Kotamraju VR, Ruoslahti E. C-end rule peptides mediate neuropilin-1-dependent cell, vascular, and tissue penetration. Proc Natl Acad Sci U S A. 2009; 106:16157–16162. [PubMed: 19805273]

4. Sugahara KN, Teesalu T, Karmali PP, Kotamraju VR, Agemy L, Girard OM, et al. Tissue-penetrating delivery of compounds and nanoparticles into tumors. Cancer Cell. 2009; 16:510–520. [PubMed: 19962669]

5. Sugahara KN, Teesalu T, Karmali PP, Kotamraju VR, Agemy L, Greenwald DR, et al. Coadministration of a tumor-penetrating peptide enhances the efficacy of cancer drugs. Science. 2010; 328:1031–1035. [PubMed: 20378772]

6. Roth L, Agemy L, Kotamraju VR, Braun G, Teesalu T, Sugahara KN, et al. Transtumoral targeting enabled by a novel neuropilin-binding peptide. Oncogene. 2012; 31:3754–3763. [PubMed: 22179825]

7. Arap W, Pasqualini R, Ruoslahti E. Cancer treatment by targeted drug delivery to tumor vasculature in a mouse model. Science. 1998; 279:377–380. [PubMed: 9430587]

8. Koivunen E, Gay DA, Ruoslahti E. Selection of peptides binding to the alpha 5 beta 1 integrin from phage display library. J Biol Chem. 1993; 268:20205–20210. [PubMed: 7690752]

9. Curnis F, Longhi R, Crippa L, Cattaneo A, Dondossola E, Bachi A, et al. Spontaneous formation of L-isoaspartate and gain of function in fibronectin. J Biol Chem. 2006; 281:36466–36476. [PubMed: 17015452]

10. Spitaleri A, Mari S, Curnis F, Traversari C, Longhi R, Bordignon C, et al. Structural basis for the interaction of isoDGR with the RGD-binding site of alphavbeta3 integrin. J Biol Chem. 2008; 283:19757–19768. [PubMed: 18480047]

11. Curnis F, Arrigoni G, Sacchi A, Fischetti L, Arap W, Pasqualini R, et al. Differential binding of drugs containing the NGR motif to CD13 isoforms in tumor vessels, epithelia, and myeloid cells. Cancer Res. 2002; 62:867–874. [PubMed: 11830545]

12. Pasqualini R, Koivunen E, Kain R, Lahdenranta J, Sakamoto M, Stryhn A, et al. Aminopeptidase N is a receptor for tumor-homing peptides and a target for inhibiting angiogenesis. Cancer Res. 2000; 60:722–727. [PubMed: 10676659]

13. Corti A, Curnis F. Tumor vasculature targeting through NGR peptide-based drug delivery systems. Curr Pharm Biotechnol. 2011; 12:1128–1134. [PubMed: 21470145]

14. Corti A, Pastorino F, Curnis F, Arap W, Ponzoni M, Pasqualini R. Targeted drug delivery and penetration into solid tumors. Med Res Rev. 2012; 32:1078–1091. [PubMed: 21287572]

15. Corti A, Curnis F, Arap W, Pasqualini R. The neovasculature homing motif NGR: more than meets the eye. Blood. 2008; 112:2628–2635. [PubMed: 18574027]

16. Curnis F, Sacchi A, Borgna L, Magni F, Gasparri A, Corti A. Enhancement of tumor necrosis factor alpha antitumor immunotherapeutic properties by targeted delivery to aminopeptidase N (CD13). Nat Biotechnol. 2000; 18:1185–1190. [PubMed: 11062439]

17. Agemy L, Sugahara KN, Kotamraju VR, Gujraty K, Girard OM, Kono Y, et al. Nanoparticle-induced vascular blockade in human prostate cancer. Blood. 2010; 116:2847–2856. [PubMed: 20587786]

18. Teesalu T, Sugahara KN, Ruoslahti E. Mapping of Vascular ZIP Codes by Phage Display. Methods Enzymol. 2012; 503:35–56. [PubMed: 22230564]

19. Curnis F, Cattaneo A, Longhi R, Sacchi A, Gasparri AM, Pastorino F, et al. Critical role of flanking residues in NGR-to-isoDGR transition and CD13/integrin receptor switching. J Biol Chem. 2010; 285:9114–9123. [PubMed: 20064928]

20. Agemy L, Friedmann-Morvinski D, Kotamraju VR, Roth L, Sugahara KN, Girard OM, et al. Targeted nanoparticle enhanced proapoptotic peptide as potential therapy for glioblastoma. Proc Natl Acad Sci U S A. 2011; 108:17450–17455. [PubMed: 21969599]

21. Mayer LD, Dougherty G, Harasym TO, Bally MB. The role of tumor-associated macrophages in the delivery of liposomal doxorubicin to solid murine fibrosarcoma tumors. J Pharmacol Exp Ther. 1997; 280:1406–1414. [PubMed: 9067330]

22. Colombo G, Curnis F, De Mori GM, Gasparri A, Longoni C, Sacchi A, et al. Structure-activity relationships of linear and cyclic peptides containing the NGR tumor-homing motif. J Biol Chem. 2002; 277:47891–47897. [PubMed: 12372830]

23. Becker PM, Waltenberger J, Yachechko R, Mirzapoiazova T, Sham JS, Lee CG, et al. Neuropilin-1 regulates vascular endothelial growth factor-mediated endothelial permeability. Circ Res. 2005; 96:1257–1265. [PubMed: 15920019]

24. Corti A, Curnis F. Isoaspartate-dependent molecular switches for integrin-ligand recognition. J Cell Sci. 2011; 124:515–522. [PubMed: 21282473]

25. Werle M, Bernkop-Schnurch A. Strategies to improve plasma half life time of peptide and protein drugs. Amino Acids. 2006; 30:351–367. [PubMed: 16622600]

26. Haspel N, Zanuy D, Nussinov R, Teesalu T, Ruoslahti E, Aleman C. Binding of a C-end rule peptide to the neuropilin-1 receptor: a molecular modeling approach. Biochemistry. 2011; 50:1755–1762. [PubMed: 21247217]

27. Jubb AM, Strickland LA, Liu SD, Mak J, Schmidt M, Koeppen H. Neuropilin-1 expression in cancer and development. J Pathol. 2012; 226:50–60. [PubMed: 22025255]

28. Laakkonen P, Porkka K, Hoffman JA, Ruoslahti E. A tumor-homing peptide with a targeting specificity related to lymphatic vessels. Nat Med. 2002; 8:751–755. [PubMed: 12053175]

29. Fogal V, Zhang L, Krajewski S, Ruoslahti E. Mitochondrial/cell-surface protein p32/gC1qR as a molecular target in tumor cells and tumor stroma. Cancer Res. 2008; 68:7210–7218. [PubMed: 18757437]

30. Ruoslahti E, Bhatia SN, Sailor MJ. Targeting of drugs and nanoparticles to tumors. J Cell Biol. 2010; 188:759–768. [PubMed: 20231381]
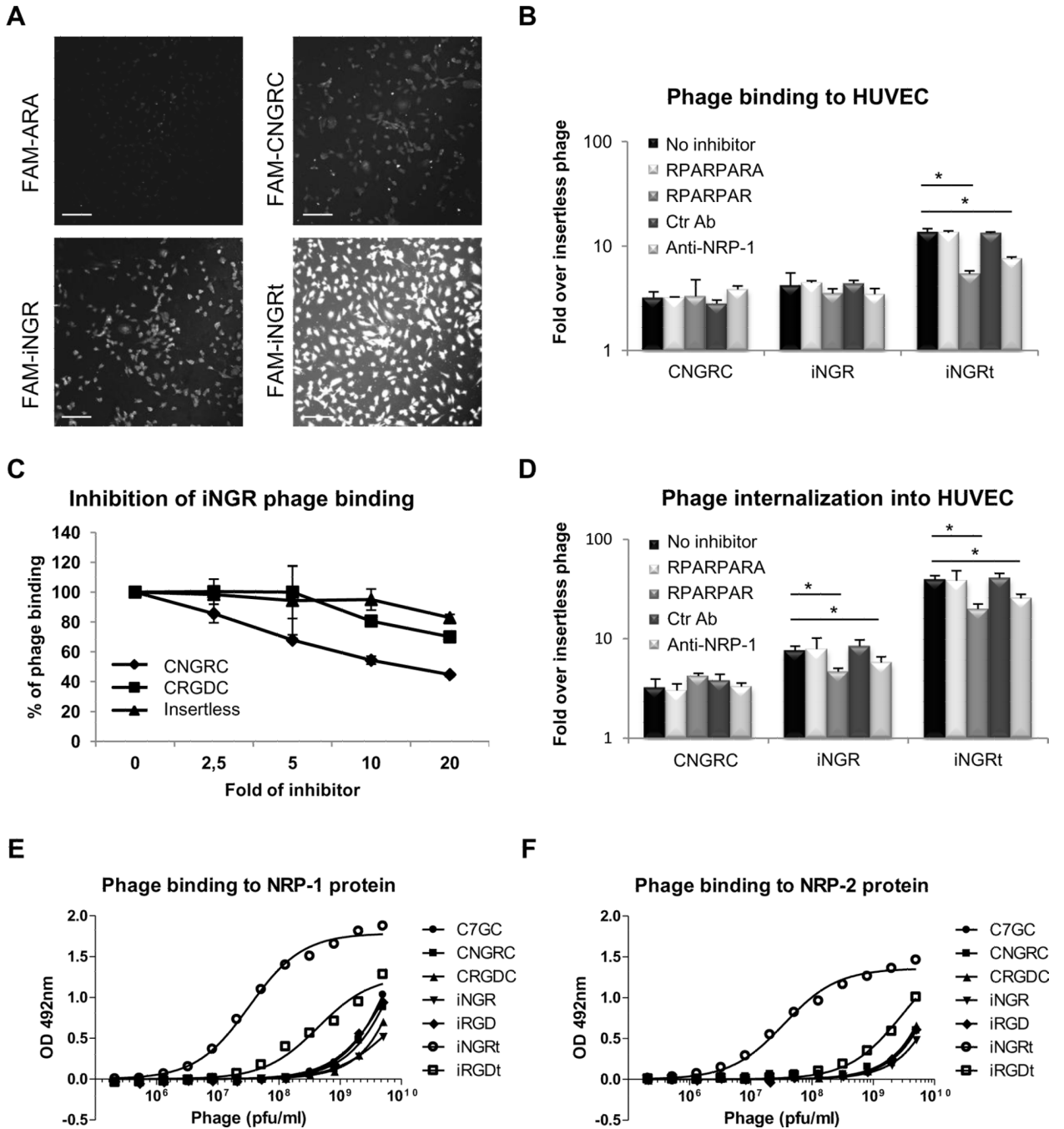
Fig. 1. iNGR shares the same receptor with CNGRC and, upon activation, strongly interacts with NRPs

(A)HUVECs were incubated for 2 hours at 4°C with FAM-labeled ARA (ARALPSQRSR; (28)), CNGRC, iNGR or iNGRt peptides. Cells were fixed and imaged with a Fluoview confocal microscope. Scale bars: 100 μm. (B and D) Tenfold excess of UV-inactivated RPARPAR or RPARPARA phage, or 1 μg/ml of control or neutralizing NRP-1 antibody was used to inhibit the binding (B) or the internalization (D) of CNGRC, iNGR or iNGRt phage in HUVECs. The results are shown as fold increase over insertless phage. * one way ANOVA < 0.05. Error bars: Standard Error. (C) Dose-dependent inhibition of iNGR phage binding to HUVECs by UV-inactivated phage. iNGR phage binding without inhibitors was

considered as 100%. Error bars: Standard Error. (E and F) Dose-dependent binding of phage to purified NRP-1 (E) or NRP-2 (F) proteins. The number of phage bound to the proteins was quantified using a combination of a rabbit anti-T7 phage antibody and an HRP-labeled goat anti-rabbit antibody.
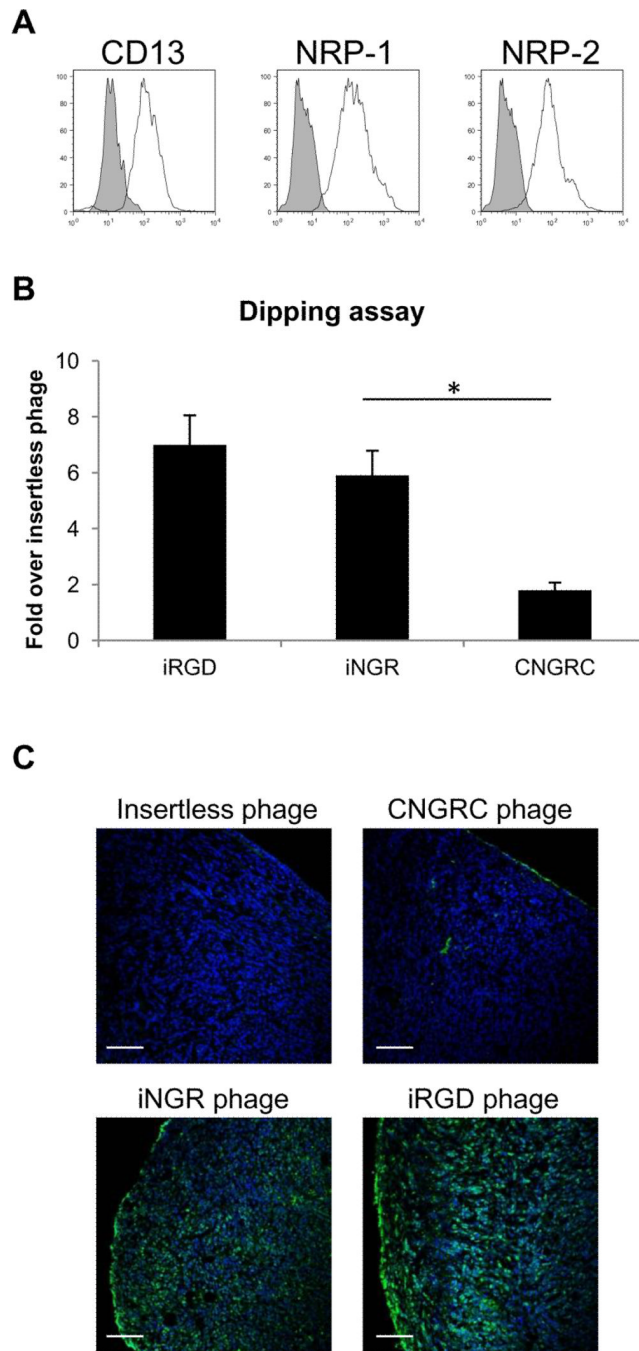
A

B

Dipping assay

C

Fig. 2. iNGR penetrates deeper to tumors than NGR
(A) Expression of CD13, NRP-1, and NRP-2 on 4T1 cells analyzed by flow cytometry. The profiles represent the values of cells stained with appropriate antibodies (solid lines) or an isotype control (shaded). (B) Explanted 4T1 tumors were incubated with insertless, CNGRC, iNGR or iRGD phage. Phage bound to the tumor surface were removed with acid wash, and the number of phage particles that penetrated into the tumors was quantified by phage titration. Results are shown as fold increase over insertless phage. Each value was normalized against tumor weight. * one way ANOVA < 0.05. Error bars: Standard Error. (C) Tumor dipping assays were performed as in (B), and frozen tumor sections were stained with an anti-T7 phage antibody (green) and DAPI (blue). Scale bars: 100μm.
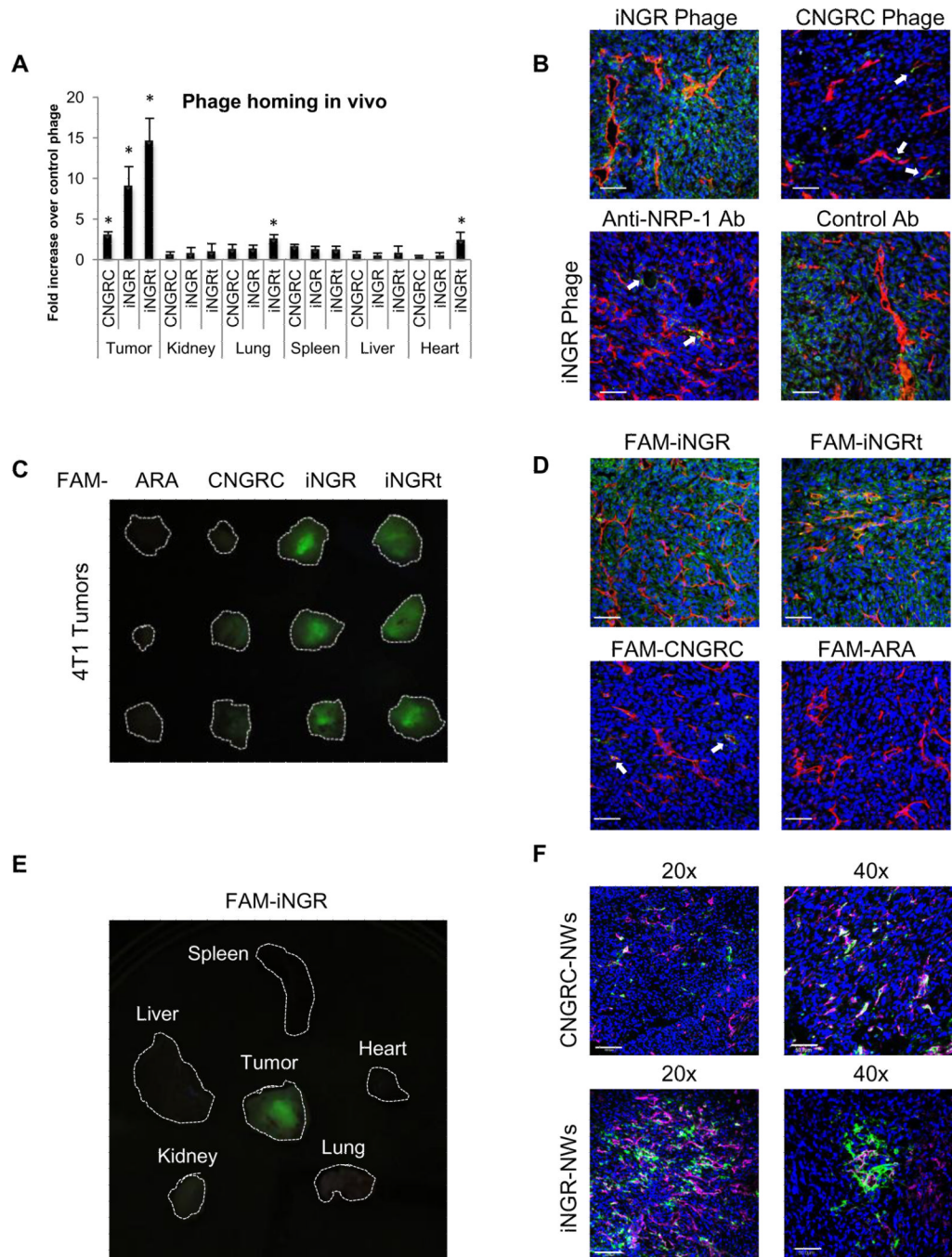
Fig. 3. Systemic iNGR selectively accumulates in and penetrates into tumors
(A-B *In vivo* phage homing to orthotopic 4T1 tumors. Phage were intravenously injected into 4T1 bearing mice and allowed to circulate for 40 minutes. After perfusion of the mice, tissues were collected and homogenized for phage titration (A) or processed for phage (green) and CD31 (red) immunostaining (B). Blue represents DAPI staining. In some cases, iNGR phage was co-injected with 50 μg of neutralizing NRP-1 antibody or rabbit IgG (B, lower panels). * one way ANOVA < 0.05. Scale bars: 50μm. Error bars: Standard Error (C-E) *In vivo* peptide homing to 4T1 tumors. One hundred micrograms of FAM-peptides (green) were intravenously injected into 4T1 bearing mice. One hour later, the mice were perfused, and tissues were collected and imaged on a UV light table (C and E). Then, the

tissues were processed for CD31 (red) and nuclei (blue) staining (D) Scale bars: 50μm. (F) *In vivo* homing of NWs to 4T1 tumors. CNGRC- or iNGR-coated NWs (green) were injected into the tail vein of 4T1 tumor mice. After 4 hours, the mice were perfused, and tumors were collected and subjected to CD31 staining (red). Blue represents DAPI staining. Confocal images at 20x and 40x magnifications are shown. Scale bars: 100μm (20x), 50μm (40x). The arrows point to blood vessels positive for phage (B) or peptide (D). Note that the iNGR phage, peptide, and NWs effectively penetrated 4T1 tumors, and that the anti-NRP-1 antibody inhibited the tumor penetration of iNGR phage.
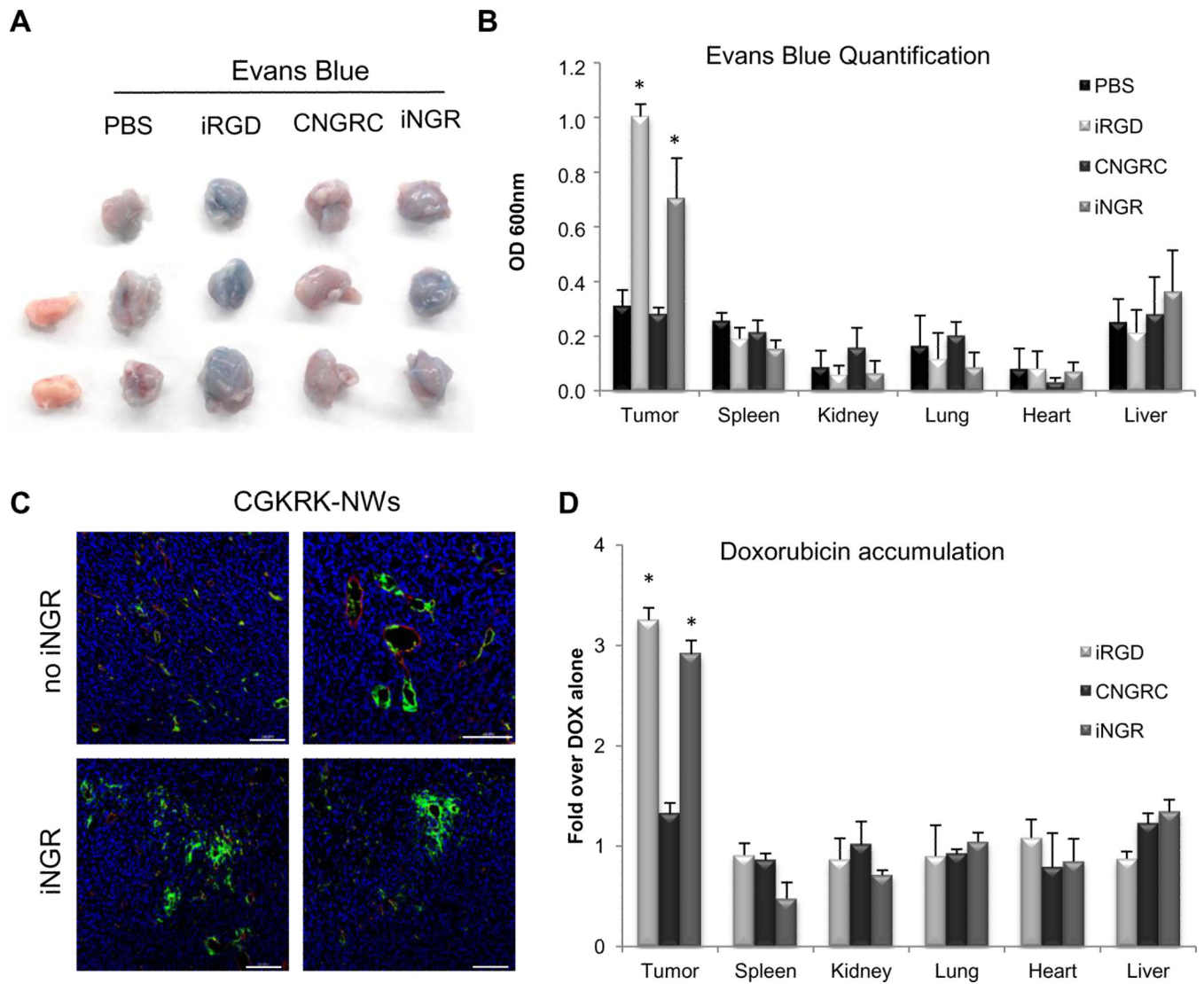
Fig. 4. iNGR triggers tumor-specific penetration of co-administered compounds
(A and B) One milligram of Evans Blue dye was intravenously co-injected with 4 μmol/kg
of peptides or PBS. After 40 minutes of circulation, the mice were extensively perfused, and
tumors were collected for imaging under white light (A). Evans blue was extracted from the
collected tumors and organs and quantified by OD_{600} measurement (B). (C) Five mg/kg of
FAM-CGKRK-conjugated NWs (green) were injected with or without 4 μmol/kg of iNGR
peptide into the tail vein of 4T1 bearing mice. After 5 hours of circulation, tumors were
collected for CD31 immunostaining (red). Blue represents DAPI staining. Two
representative images of three tumors are shown. Scale bars: 100μm. (D) Ten mg/kg of
DOX was intravenously co-injected with 4 μmol/kg of the indicated peptides in 4T1-bearing
mice. After 1 hour of circulation, the mice were extensively perfused, and the tissues were
collected for DOX quantification. Results are shown as fold increase over DOX alone. * one
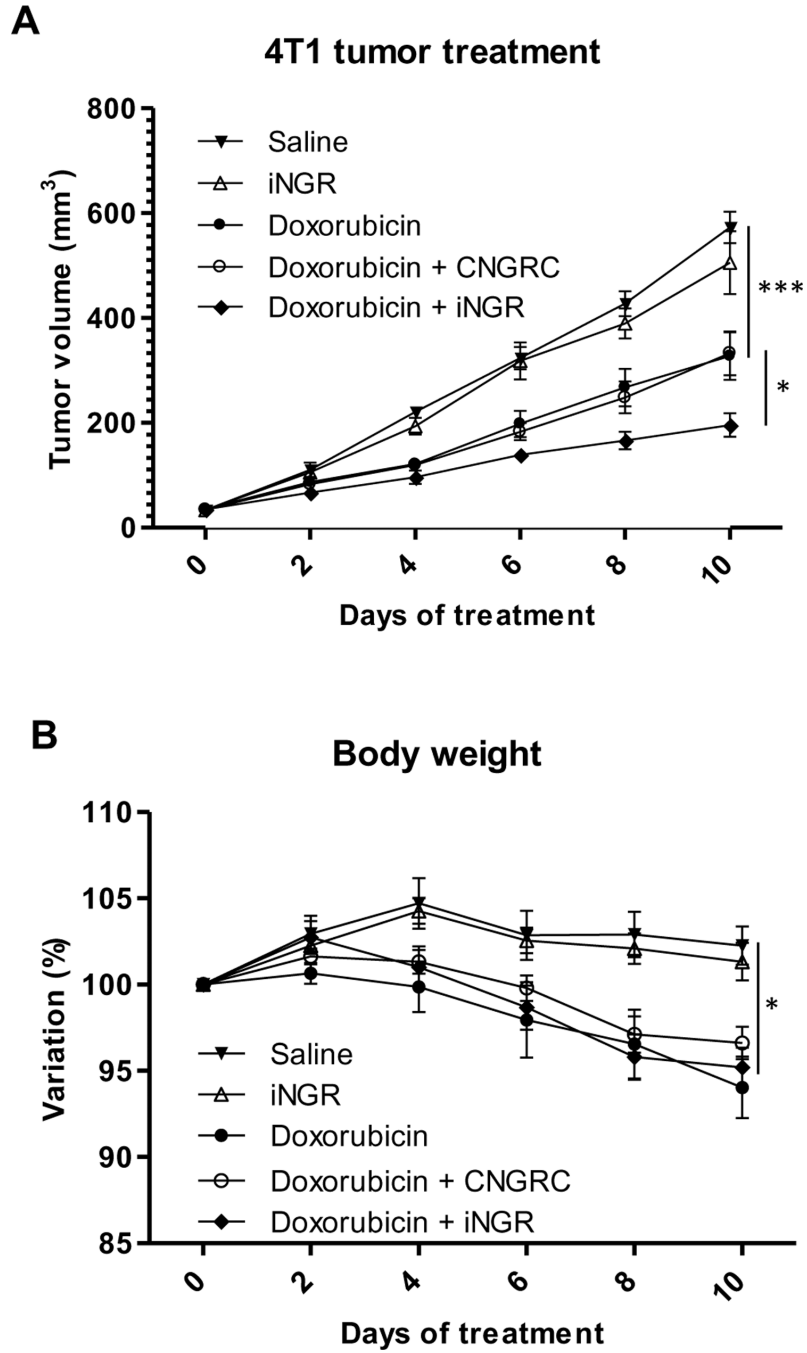way ANOVA < 0.05. Error bars: Standard Error.

A

B

Fig. 5. iNGR enhances efficacy of anticancer drugs without affecting side effects
(A) Mice bearing orthotopic 4T1 tumors were treated every other day with PBS or 3 mg/kg
of DOX combined with 4 μmol/kg of CNGRC or iNGR peptide. Tumor growth was
assessed every other day. (B) Body weight changes of the tumor mice from the treatment
studies in (A). Percent body weight shift is shown. * two-way ANOVA < 0.05. *** two-way
ANOVA < 0.001. Error bars: Standard Error.